ELSEVIER

Electroencephalography and clinical Neurophysiology 103 (1997) 499–515

EEG coherency I: statistics, reference electrode, volume conduction, Laplacians, cortical imaging, and interpretation at multiple scales

Paul L. Nunez[a,b,*], Ramesh Srinivasan[b,c], Andrew F. Westdorp[a,d], Ranjith S. Wijesinghe[a,g], Don M. Tucker[b,c], Richard B. Silberstein[e,f], Peter J. Cadusch[e,f]

[a]*Brain Physics Group, Department of Biomedical Engineering, Tulane University, New Orleans, LA, USA*
[b]*Electrical Geodesics, Inc., Riverfront Research Park, Eugene, OR, USA*
[c]*Department of Psychology, University of Oregon, Eugene, OR, USA*
[d]*National Institute of Alcohol Abuse and Alcoholism, National Institutes of Health, Washington, DC, USA*
[e]*Brain Sciences Institute, Melbourne, Australia*
[f]*School of Biophysics and Electrical Engineering, Swinburne University of Technology, Melbourne, Australia*
[g]*Department of Neurology, Louisiana State University Medical School, New Orleans, LA, USA*

Accepted for publication: 23 May 1997

Abstract

Several methodological issues which impact experimental design and physiological interpretations in EEG coherence studies are considered, including reference electrode and volume conduction contributions to erroneous coherence estimates. A new measure, 'reduced coherency', is introduced as the difference between measured coherency and the coherency expected from uncorrelated neocortical sources, based on simulations and analytic-statistical studies with a volume conductor model. The concept of reduced coherency is shown to be in semi-quantitative agreement with experimental EEG data. The impact of volume conduction on statistical confidence intervals for coherence estimates is discussed. Conventional reference, average reference, bipolar, Laplacian, and cortical image coherencies are shown to be partly independent measures of neocortical dynamic function at different spatial scales, due to each method's unique spatial filtering of intracranial source activity. © 1997 Elsevier Science Ireland Ltd.

Keywords: Coherence; Spline-Laplacian; Cortical image

1. Medical and cognitive coherency studies

Scalp recorded EEG coherence and covariance are large scale measures of functional interrelations between pairs of neocortical regions. These measures are often closely correlated with cognitive or behavioral measures. For example, evoked potential covariance patterns, including the contingent negative variation and P300, are dependent on task performance (Gevins and Cutillo, 1986, 1995). Covariance between waveforms is a time-domain measure normally applied to evoked or event-related potentials. Covariance normalized by the product of individual variances is called the correlation function coefficient (Bendat and Piersol, 1986); it is a function of the lag time between signals. For example, an evoked potential waveform at one scalp location may be correlated with another location only after some time delay, perhaps associated with signal propagation.

This paper focuses on the frequency-domain measure coherence rather than covariance, although many of the ideas apply to both measures. The relationships between normalized and unnormalized measures are shown in Table 1, indicating that coherence (also called 'coherency' or 'squared coherency') is the cross spectral density function normalized by individual auto spectral density functions (also called 'power spectra'). Coherency is a

* Corresponding author.

PII S0013-4694(97)00066-7

Table 1

Relationships between normalized and unnormalized measures

	Time-domain transient EPs	Frequency-domain EEG, steady-state EPs
Unnormalized	Covariance	Cross-spectral density
Normalized	Correlation function coefficient	Coherence

correlation function (magnitude between zero and one) expressed as a function of frequency.

Scalp potential coherency studies have included studies of intelligence measures in children (Thatcher and Walker, 1985), regional changes during cognition (Tucker et al., 1985; Pfurtscheller and Berghold, 1989; Nunez and Pilgreen, 1991; Nunez, 1995; Andrew and Pfurtscheller, 1995, 1996a), spatial tasks (Rappelsberger and Petsche, 1988), listening to music (Petsche et al., 1993), maturation of coherence patterns (Thatcher et al., 1986; Marosi et al., 1992), agenesis of corpus callosum (Nielsen et al., 1993; Koeda et al., 1995; Pilgreen, 1995), and split-brain patients (Nunez, 1981). By contrast to relatively high coherencies at perhaps 5–20 cm electrode separations typically obtained with scalp recordings, intracranial, interictal coherence in epileptic patients is normally much smaller at such large distances (Gotman, 1987; Lieb et al., 1987). For example, subdural coherence measured with 2 mm diameter electrodes typically falls to zero at all frequencies for electrode separations greater than about 2 cm (Bullock et al., 1995a,b), whereas alpha rhythm scalp coherencies are often in the 0.4–0.9 range over anterior-posterior distances as large as 20 cm (Nunez, 1995). In fact, scalp coherencies often do not fall off simply with distance (Thatcher et al., 1986; Nunez, 1995). For example, alpha coherence of occipital to progressively more frontal locations shows a monotonic coherency fall-off towards central regions, but a progressive coherence increase from central to frontal cortex (Srinivasan et al., 1997).

These large differences between scalp and intracranial coherency magnitudes result partly from volume conduction and reference electrode effects (Nunez, 1981, 1995). Here, we suggest ways to reduce such errors. However, even when coherency due to volume conduction is entirely removed, measured scalp coherency may remain much higher than intracranial coherency. This apparently occurs because the large and intermediate scale coherencies measured from scalp, and intracranial recordings using electrodes of different size, provide distinct, partly independent measures of multiscale neocortical dynamic function.

In order to illustrate differences between time- and frequency-domain studies and the important issue of measurement scale, we consider a metaphor of dynamic human activity. In this fable, persons correspond to neurons, cities to macrocolumns, large metropolitan areas to perhaps 100 macrocolumns, and the earth's surface to neocortex. We might follow correlations between individual persons (pairs of microelectrode recordings), between activity averaged over large human populations (pairs of scalp EEG electrodes), or anything in between. If we follow sleep/waking measures, the correlation function coefficients between population centers will be large at time lags corresponding to the time differences between centers. The corresponding coherency will be large at frequencies near 1/24 h. Since most people sleep during approximately the same local times, both of these measures will be relatively independent of spatial scale. However, consider another human activity, say rice consumption. Correlation function coefficients and coherencies between large centers, say San Francisco and Tokyo, could be low at all time lags and frequencies. At the same time, correlations at smaller scales might be much higher, for example between San Francisco's China Town and a similar sized part of Tokyo. The corresponding correlations between even smaller groups could be quite variable with both frequency and scale, for example in populations of irregular rice eaters. While unprocessed (reference) EEG coherence (involving pairs of regions with areas greater than 100 cm^2) is somewhat analogous to coherency between large metropolitan areas, spline-Laplacian and cortical image coherency (areas of perhaps 10–30 cm^2) are analogous to coherency between somewhat smaller regions with the same centers.

In order to illustrate the very large spatial scale associated with raw scalp potentials, consider an example simulation in which radial dipole sources are uniformly distributed over the entire inner hemisphere (dura) of a 3 sphere model of the head (Nunez, 1986). The simulation illustrated in Fig. 1 predicts that only about half the contribution to the outer surface (scalp) potential comes from sources within a 3 cm radius of the 'recording' electrode (even assuming no reference electrode contribution). This occurs because a large number of distant sources can produce large local potentials when the potential due to each dipole falls off relatively slowly with scalp distance. By contrast, nearly all contributions to cortical image or spline-Laplacian measures come from sources within the same 3 cm circle. Distributions of cortical sources need not be uniform so that the idealized model in Fig. 1 is only a crude approximation. In actual EEG practice, the circle containing half the contribution to local scalp potential could be either larger or smaller than 3 cm. However, the simulation demonstrates the generally large non-local character of raw scalp potentials. It shows that an idea implicit in some publications—sources close to each electrode make the major contribution to scalp potential when a 'quiet reference' is used—is often quite wrong. Raw potential, spline-Laplacian, and cortical image coherency measures generally apply to different spatial scales of neocortical dynamic function. The implications of these ideas for obtaining robust coherency estimates in future clinical and cognitive studies is discussed in the following sections of this paper (referred to as Part I). An experimental EEG study designed to illustrate these ideas

is outlined in a following paper (Nunez et al., 1997; referred to as Part II).

2. Coherency estimates from simulated waveforms

Coherence is a quantitative measure of the phase consistency between two signals. Consider, for example, coherence between voltages at two nodes in a linear, noise-free electric circuit. Whereas each node voltage will oscillate at the AC generator frequency with generally different phase, phase differences remain fixed over time. Coherencies between all paired voltages in the circuit are equal to one in such linear circuits. Coherencies of less than one occur only if the circuit has non-linear elements or because of external influences (including, but not limited to, noise). Thus coherencies measured between separate electric circuits or between distinct scalp locations provide measures of mutual influences or long-range 'synchrony', but the magnitudes of such influences in complex, non-linear dynamic systems can be quite different at different frequencies or different spatial scales. Both experimental data and theoretical EEG studies suggest that neocortex can exhibit global dynamics (more dominant functional integration) in some frequency ranges (often near 10 Hz) while simultaneously showing more local behavior (dominant functional segregation) at other frequencies (perhaps near 40 Hz; Nunez, 1989, 1995; Pfurtscheller and Neuper, 1992; de Munck et al., 1992; Pfurtscheller et al., 1994; Andrew and Pfurtscheller, 1996a,b).

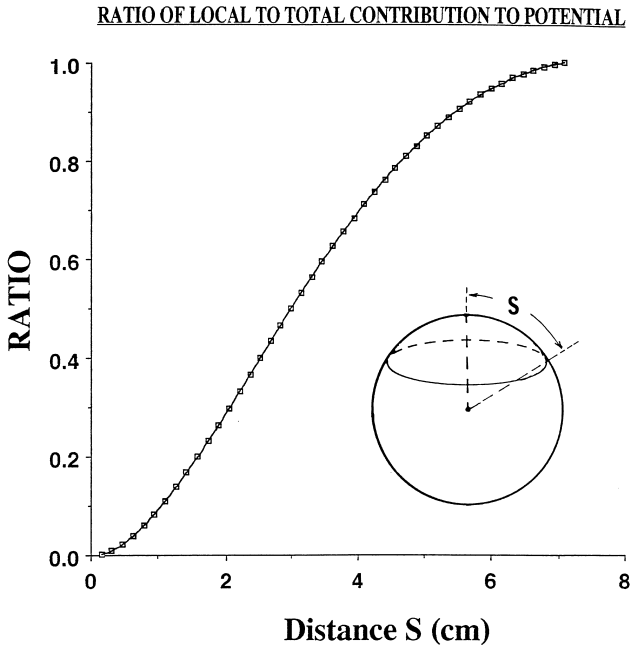

Fig. 1. A simulation using a volume conductor model of the head consisting of three concentric spherical surfaces (brain, skull, and scalp) in which radial dipole sources of fixed strength are assumed to be uniformly distributed over the inner sphere (dura). Outer surface (scalp) potentials are calculated at the 'north pole' ($\Theta = 0°$, $\Phi = 0°$ in standard spherical coordinates). Potentials are assumed to be generated in dipole layers forming symmetric spherical caps of size s (measured along the outer surface, as shown). Such potentials were expressed earlier as infinite sums of Legendre polynomials (Nunez, 1986). The ratios of outer surface (scalp) potentials due to all sources within caps of size s to potentials generated by the entire upper surface ($\Theta = 90°$ or $s = 14.5$ cm) are plotted versus distances. Given this idealized assumption of uniform, cortical gyri sources, the simulation predicts that less than 5% of measured scalp potential comes from sources directly under a 1 cm diameter 'recording' electrode ($s = 0.5$ cm), and about half the contribution comes from sources within a 3 cm radius of the electrode center. More than 95% of the potential is generated by sources within 6 cm (assuming no reference electrode contribution).

An example 1 s waveform composed of 3 frequency components (5, 12, 20 Hz) of unequal amplitudes (5, 12, 1) and phases plus random noise (amplitude = 15) is shown in Fig. 2a. Suppose that we wish to measure mutual influences between this signal and a similar signal also composed of the same 3 frequency components. The amplitude spectrum for one waveform based on a 1 min record is shown in Fig. 2b; the amplitude spectrum for the second waveform is nearly identical showing that both waveforms have contributions at 5, 12, and 20 Hz. In our simulation, we randomly varied the relative phases (from each 1 s epoch to the next) between the two waveforms according to frequency, i.e. 5 Hz (−18 to +18°), 12 Hz (−180 to +180°), 20 Hz (constant phase). The resulting coherency spectrum estimate, based on 60 1 s epochs (shown in Fig. 2c), indicates that coherencies are relatively high at 5 and 20 Hz, but essentially zero at all other frequencies, including 12 Hz where amplitude is relatively high. Furthermore, amplitude is largest at 12 Hz, but coherency is largest at 20 Hz. Clearly, amplitude (or power) and coherency are generally independent measures of waveforms, although neocortical dynamics and/or volume conduction may force relations between them. For example, increased EEG scalp amplitude is typically associated with increased local 'synchrony' (increased coherence of local current sources, within a few centimeters), but this can occur independently of longer range coherence changes which may have minimal effect on amplitude.

3. Erroneous coherency estimates

Here we outline possible origins of discrepancies between coherency obtained from scalp potentials and the underlying neural source coherency. Some differences between scalp potential and source coherency measures are unavoidable and do not necessarily invalidate EEG cognitive or medical studies of robust coherency changes between brain states. However, when discrepancies between measured and underlying source coherencies are too large or physiological interpretation is inaccurate, problems may arise, including:

1. Failure to choose the coherency measures exhibiting the largest differences between brain states or between patient populations.

2. Difficulty in making comparisons with other laboratories using slightly different experimental methods (e.g. different reference).
3. Basing new experiments on erroneous physiological interpretations of coherency estimates.
4. Applying inappropriate statistical tests.

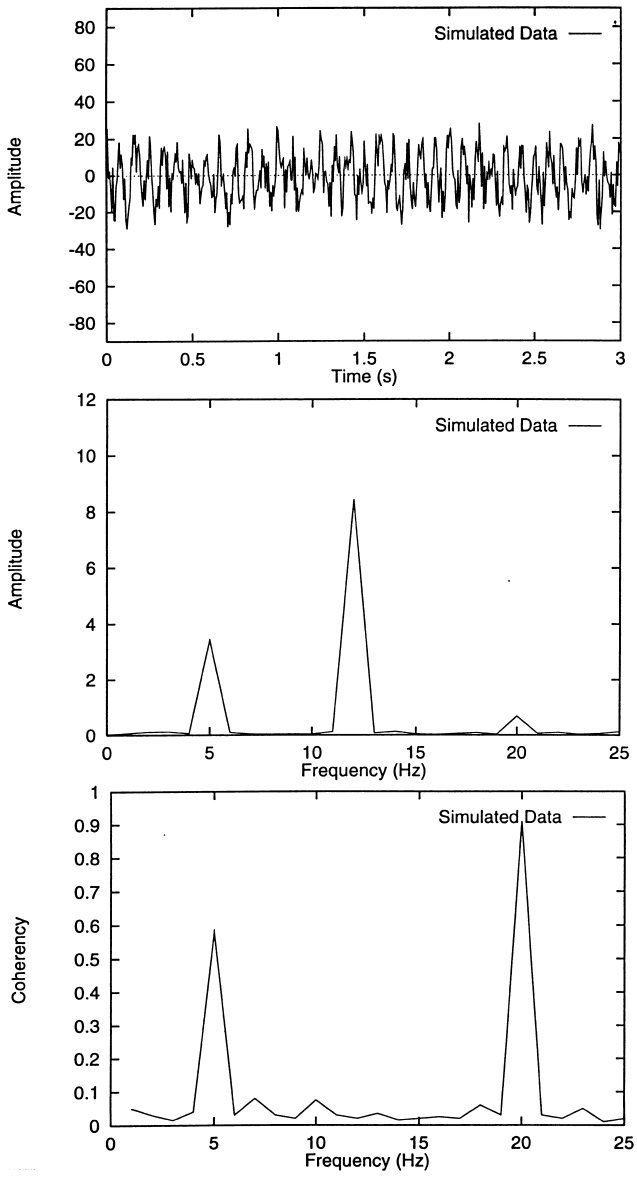

Fig. 2. (a) An example 1 s waveform composed of frequency components 5, 12, and 20 Hz with unequal amplitudes (5, 12, and 1) and phases, plus random noise (amplitude 15) is shown. (b) Amplitude spectra for the two waveforms are essentially identical; only one is shown. Relative phases were varied randomly from each 1 s epoch to the next according to frequency, i.e. 5 Hz (−18° to +18°), 12 Hz (−180° to +180° or random phase), and 20 Hz (constant phase). (c) The resulting coherency spectrum estimate for the paired waveforms is based on 60 1 s epochs. Coherency at each frequency depends on epoch-to-epoch phase consistency, it is largest at 20 Hz where the phase difference between the two waveforms is constant and zero at frequencies with random phase, independent of waveform magnitudes.

Erroneous EEG coherence estimates may be caused by:

1. Statistical errors if the number of epochs averaged is too small (erroneous high or low coherence).
2. Reference electrode effects (often erroneous high coherence, but erroneous low coherence at some sites may also occur).
3. Volume conduction (erroneous high coherence).
4. High pass filtering of genuine cortical signals by Laplacian or cortical imaging algorithms (erroneous low coherence).
5. Laplacian or cortical imaging algorithm effects (possible erroneous high coherence; however, the errors are apparently small with accurate algorithms).

We can never know actual coherencies for experimental data which depend on the unknown probability density functions of associated stochastic processes (Katznelson, 1982; Bendat and Piersol, 1986; de Munck et al., 1992), only estimates are possible (as in the case of all correlation coefficients). We chose to divide our EEG record of length L into N epochs. In this manner a frequency resolution of $Df = N/L$ was obtained; i.e. Df is the bandwidth applicable to each coherency estimate. For example, the 1 min records of Fig. 2 were divided into 60 1 s epochs for Fourier analysis yielding 1.0 Hz frequency resolution. If these same records had been divided into 120 0.5 s epochs, the frequency resolution would be 2.0 Hz. For example, the coherency estimate at 5 Hz in Fig. 2 applies roughly to the band 4.5–5.5 Hz, whereas the same records would yield estimates in the band 4.0–6.0 Hz if 0.5 s epochs were used. With this broader frequency resolution, we have twice as many epochs to average in a record of fixed length, thereby obtaining higher confidence in coherence estimates.

Each epoch, n, of channel i yields the complex Fourier transform $X_{in}(f)$. The single epoch 'power spectrum' (auto spectral density function) is:

$$G_{in}(f) = X_{in}(f)X_{in}^{*}(f) \tag{1}$$

and the cross spectral density function for channels i and j is:

$$G_{ijn}(f) = X_{in}(f)X_{jn}^{*}(f) \tag{2}$$

where * indicates the complex conjugate. These equations can provide accurate estimates only if many epochs (N) are averaged; i.e. the cross spectral density function estimate is:

$$\hat{G}_{ij}(f) = \frac{1}{N}\sum_{n=1}^{N} G_{ijn}(f) \tag{3}$$

with a similar expression for the estimated power spectrum $G_i(f)$ for each channel i. The coherency estimate based on N epochs is:

$$\hat{\gamma}_{ij}^{2}(f) = \frac{|\hat{G}_{ij}(f)|^2}{\hat{G}_i(f)\hat{G}_j(f)} \tag{4}$$

The 95% confidence interval for either power or coherence estimates can be expressed as (Bendat and Piersol, 1986):

$$\frac{\hat{G}(f)}{1+2e} \le G(f) \le \frac{\hat{G}(f)}{1-2e} \tag{5}$$

This equation applies to auto or cross spectral density and coherency. The confidence interval depends on the error term e (normalized RMS error). For spectral density function estimates based on non-overlapping epochs (assumed to be statistically independent), the error may be estimated by:

$$e_G = \frac{1}{\sqrt{N}} \tag{6}$$

if the epoch number is greater than about 25. In addition to this RMS error, there is a bias error which is relatively small for this many epochs (Bendat and Piersol, 1986) and is neglected here. The error term for coherence estimates depends on coherence itself; it may be estimated using estimated coherence provided the error is small, say less than about 0.2.

$$e_{\gamma^2} \cong \sqrt{2/N}\ \frac{1-\hat{\gamma}^2}{|\hat{\gamma}|} \tag{7}$$

For any fixed data record of length L, there is always a compromise between confidence interval eqn (5) and frequency resolution when coherence is based on fast Fourier transform methods. Alternate coherence methods, which may be applied to short EEG records, involve somewhat different compromises (Schack and Krause 1995; Schack et al., 1996).

As an example, we use the records of Fig. 2. With $N = 60$ epochs, the spectral density function error from eqn (6) is about 0.13. If our spectral density estimate at some frequency f_0 is $G(f_0) = 10.0$, the 95% confidence interval for the estimate is:

$$7.9 \le G(f_0) \le 13.5 \tag{8}$$

which applies to the band $f_0 \pm 0.5$ Hz. The corresponding 95% confidence intervals for several coherency estimates approximated from eqns (5), () and (7) are:

$$\hat{\gamma}^2 = 0.8 \quad 0.7 \le \gamma^2 \le 0.9 \tag{9}$$

$$\hat{\gamma}^2 = 0.5 \quad 0.4 \le \gamma^2 \le 0.7$$

$$\hat{\gamma}^2 = 0.2 \quad 0.1 \le \gamma^2 \le 0.6$$

Here the last estimate is very crude since the RMS error given by eqn (7) is 0.33 and eqn (7) is valid only for small errors. However, the confidence interval is qualitatively correct. Thus moderate to high coherency estimates based on 60 epoch averages indicate high probabilities that two signals are indeed correlated at a particular frequency. However, estimated coherencies in the 0.05–0.1 range (based on 60 epochs) could easily occur in uncorrelated signals, as also implied by Fig. 2c. With smaller numbers of epochs to average, due to shorter record lengths, narrower frequency resolution, or both, only higher estimated coherencies can be reliably associated with genuine signal correlation using the usual fast Fourier transform methods.

4. Reference electrode and volume conduction effects

The simplistic distinction between ‘recording’ and ‘reference’ electrode is valid only when we know in advance that all current sources are close to the recording electrode (Rush and Driscoll, 1969; Nunez, 1981). However, the more usual EEG study involves distributed sources and unknown locations (Nunez, 1995). We have simulated distributed sources in head volume conductor models to demonstrate that scalp potentials are generally reference-dependent, even when there are no sources close to the reference electrode (Nunez et al., 1991). This suggests that the common concept of a ‘quiet reference’ is of very limited use to EEG.

In order to estimate the effects of volume conduction and reference electrode on various coherence measures, we used a 3 concentric spheres model of the head containing 4200 uncorrelated, radial dipole sources at the approximate depth (1.4 cm) of cortical gyri. Outer surface (scalp) potentials are calculated at 64 locations, matching electrode positions used in the experimental study described in Part II (Nunez et al., 1997). Thus, we obtain potentials V_i and V_j for each electrode pair ($64 \times 63/2 = 2016$) separated by some surface distance. The calculations are repeated for 60 different distributions of the 4200 random sources, thereby yielding scatter plots of V_i versus V_j for each electrode separation. Simple linear regression methods then provide plots of scalp potential correlation coefficients squared (analogous to coherency) versus electrode separation. These simulations are similar to earlier studies (Nunez, 1995) involving 4200 sources and 500 source distributions, but here we chose 60 source distributions to match experimental coherencies calculated with 60 averages, as described in Part II (Nunez et al., 1997). The results of these separate simulation studies are similar but, as expected, correlations obtained with more random source distributions have less scatter. The proposed close connection of simulated, squared correlation coefficient to experimental coherency is partly based on the fact that passive current spread in the head volume conductor is independent of frequency. This issue is discussed in more detail in a later section.

The simulated, squared correlation coefficient is plotted versus surface distance in Fig. 3a for the case of potentials measured with respect to a reference at the top of the sphere (representing a Cz reference). This is clearly a poor reference choice since Cz lies within the array. The correlations in Fig. 3a can be large at large distances due to a combination of volume conduction and reference electrode effects. Fig. 3b shows the corresponding fall-off of correlation for a reference at the bottom of the sphere. This corresponds only

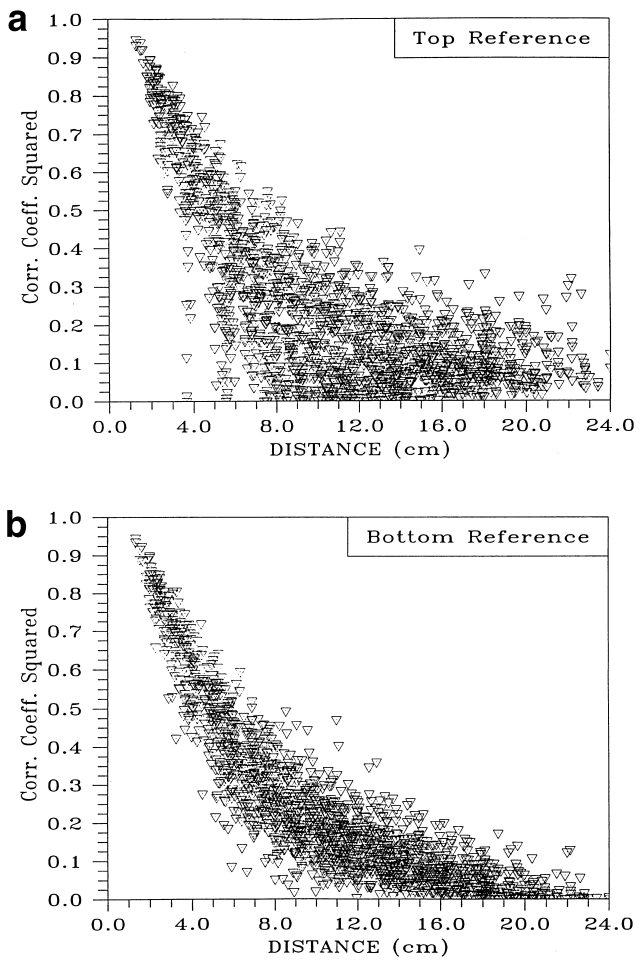

Fig. 3. (a) Simulated, squared correlation coefficients of outer surface potentials are plotted versus surface distance for the case of a reference at the top of the 3 sphere head model (representing a Cz reference). Sources are assumed to be 4200 radial dipoles uniformly distributed over the upper surface of the inner sphere, similar to the largest spherical cap of Fig. 1. However, here the sources are uncorrelated (strengths vary randomly in magnitude and polarity) so that 'scalp' potential non-zero correlations are due only to statistical fluctuations (for 60 averages), volume conduction, and reference electrode effects. Potentials are calculated at 64 'scalp' locations which correspond to actual electrode locations used in the 64 channel EEG data discussed in Nunez et al. (1997). (b) Similar to (a), except a reference on the bottom of the sphere is assumed (crudely representing a neck reference).

crudely to a neck reference since the volume conductor model consists only of concentric spherical surfaces. The large correlations at small and moderate distances (<10–12 cm) are due only to the passive spread of currents in the volume conductor, which originate from uncorrelated sources. At larger distances this effect is relatively small. If the number of source distributions is 500 (rather than 60), the squared correlations are all less than 0.1 at distances greater than 12 cm (Nunez, 1995). Since it is not possible to accurately predict reference or volume conductor effects on scalp coherence estimates without both an accurate volume conductor model and prior knowledge of all source locations, we suggest that different combinations of the following procedures may be appropriate for EEG coherence studies:

(1) Use of a non-cephalic reference to estimate large scale coherency. While this choice will not entirely eliminate reference contributions to coherence, errors should be smaller than if single ear or mastoid references are used. Another possible choice is digitally linked ears. That is, reference one ear (V_1), with potential between the two ears also recorded ($V_2 - V_1$) with an extra data channel so that scalp potentials (V_S) refer to the average potential of the two ears:

$$(V_S - V_1) - \frac{1}{2}(V_2 - V_1) = V_S - \frac{1}{2}(V_1 + V_2) = V_S - V_R \qquad (10)$$

The simulated, squared correlations fall-off for digitally linked ears are shown in Fig. 4a. At distances roughly in the 6–18 cm range, the correlations fall off faster than the bottom reference of Fig. 3b; however, paired sites close to the 'ear' locations (approximately 4 cm) yield erroneous high correlations at 18–24 cm. An experimental study of the effect of different references on EEG coherence is qualitatively consistent with the simulations shown in Figs. 3 and 4, and provides some support for the digitally linked ears or mastoid reference (Essl and Rappelsberger, 1996).

Note that the use of digitally linked ears is quite different from physically linking the ears, for which the reference potential (V_R) on the wire connecting the two ears is (Nunez, 1991):

$$V_R = \frac{R_2 V_1 + R_1 V_2}{R_1 + R_2} \qquad (11)$$

V_R can approximate the average ear potentials only if the two ear electrode contact impedances (R_1 and R_2) are nearly equal. But, electrode impedances are typically checked only to make sure they are less than about 5 kΩ. Thus, this procedure introduces a random element into EEG studies, in which references in different subjects may be unbalanced to either the right or the left (Nunez et al., 1991). Furthermore, if R_1 and R_2 are made very small, there is some chance of a significant shorting effect, thereby altering natural current paths in the scalp (Katznelson, 1981), although this later effect is probably small in most studies (Miller et al., 1991).

(2) Calculate coherencies from average reference data. This procedure eliminates coherency contributions at zero spatial frequency which are strongly influenced by volume conduction, but could introduce biases in coherence estimates if the spatial extent and number of electrodes are too small (Fein et al., 1988). The simulated, squared correlation coefficients for average reference potentials are shown in Fig. 4b. The correlations fall off much faster than either bottom or digitally linked ear references at small to moderate distances (roughly less than 10 cm.); however, correlations tend to rise at distances in the 10–24 cm range. The correlation increase at large distances results partly from the known behavior of superficial dipoles

in the 3 sphere model. That is, outer surface potential falls off to zero and then changes sign at very large distances; i.e. the magnitude then increases slightly with distance (Nunez, 1981). This behavior is also observed in simulations with potentials calculated with respect to infinity, which is expected since the average reference potential is typically close to zero when many and widespread electrodes are used. Also, the U-shaped plot of Fig. 4b is obtained in average-referenced experimental data when source correlations are apparently low, as shown in a later section and in Part II (Nunez et al., 1997).

(3) Calculate coherencies based on pairs of closely spaced bipolar electrodes (2–3 cm apart). This eliminates all reference electrode and most volume conduction effects when distances between bipolar midpoints are greater than about 4–5 cm (Nunez, 1995; Srinivasan et al., 1996, 1997), but

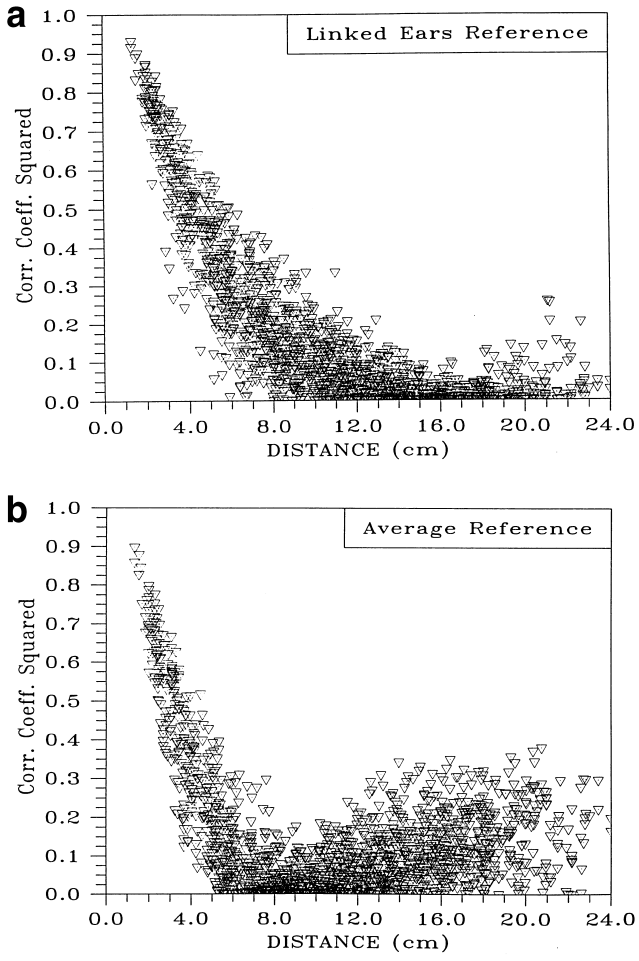

Fig. 4. (a) Simulated, squared correlation coefficients (simulating EEG coherency) are plotted versus surface distance as in Fig. 3, except potentials are here referenced to the average of potentials at $\Theta = 90°$, $\Phi = +90°$ and $-90°$ (representing two ear locations within about 4 cm of the closest sources). Electrode pairs close to references yield higher correlations due to reference contributions, as shown for electrode separations near 25 cm. This is a appropriate simulation of digitally (but not physically) linked ears or mastoids references. (b) Similar to (a) except potentials are calculated with respect to the average potential of all 64 surface potentials in order to simulate the standard EEG average reference recording.

coherence estimates are likely to be sensitive to orientations of bipolar axes due to anisotropic volume conduction, EEG dynamics (including but not limited to tangential sources), or both.

(4) Base coherency estimates on nearest-neighbor (e.g. Hjorth) Laplacians. While this approach provides very crude Laplacian estimates, it does eliminate all reference and most volume condition effect at distances a little longer than inter-electrode spacing (Nunez, 1981; Nunez and Pilgreen, 1991). However, Hjorth coherence estimates generally will also be sensitive to relative electrode orientations (Nunez et al., unpublished results, 1987).

(5) Base coherency estimates on global spline-Laplacian or cortical imaging algorithms. These methods provide estimates of local dura potential (Gevins and Cutillo, 1986, 1995; Perrin et al., 1987, 1989; Nunez, 1988, 1995; Gevins et al., 1991; Sidman, 1991; Le and Gevins, 1993; Babiloni et al., 1995, 1996; Srinivasan et al., 1996, 1997). They probably remove nearly all volume conduction errors at distances greater than a few centimeters and, because of their spatial filtering properties, apply to coherency averaged over neural sources in much smaller cortical regions. Thus, they provide partly independent measures of neocortical dynamic function at intermediate spatial scales. Global splines have been implicated with erroneous high coherency estimates (Biggins et al., 1991); however, both our simulations and studies of alpha rhythm with 3D splines (rather than the spherical splines used by the Biggins group) suggest that such effects are very small at scalp distances greater than about 3 or 4 cm, with the possible exception of locations near the edge of the electrode array.

The effects of volume conduction on cortical image and spline-Laplacian coherency due to uncorrelated cortical sources are estimated with the simulated, squared correlation coefficients shown in Fig. 5. Most of the squared correlations are less than 0.1 at distances greater than 4 cm. When 500 (rather than 60) source distributions are simulated, nearly all such squared correlations are less than 0.05. The cortical image algorithm used here contains a smoothing parameter and obtains slightly smoother estimates of cortical potential than the spline-Laplacian. This accounts for the relatively large cortical image correlations at distances less than 4.0 cm (Fig. 5a), which are not obtained with the spline-Laplacian (Fig. 5b). When smaller smoothing parameters are used, cortical image and spline-Laplacians yield similar estimates. Comparison of Fig. 5 with the various reference potential simulations of Figs. 3 and 4 may suggest that cortical image and spline-Laplacian coherency provide far more accurate representations of underlying source coherency than any of the reference coherencies (or even coherencies calculated with respect to 'true' potentials at infinity). While this may be correct for many neocortical dynamic behaviors, several caveats are required. The first is that we have only been able to assess the accuracies of cortical image and spline-Laplacian estimates of cortical potential in simulations and to show they are self-

consistent when used with experimental data. Secondly, these methods may filter out the effects of sources with very low spatial frequencies, thereby providing erroneous low coherency estimates as discussed in the next section.

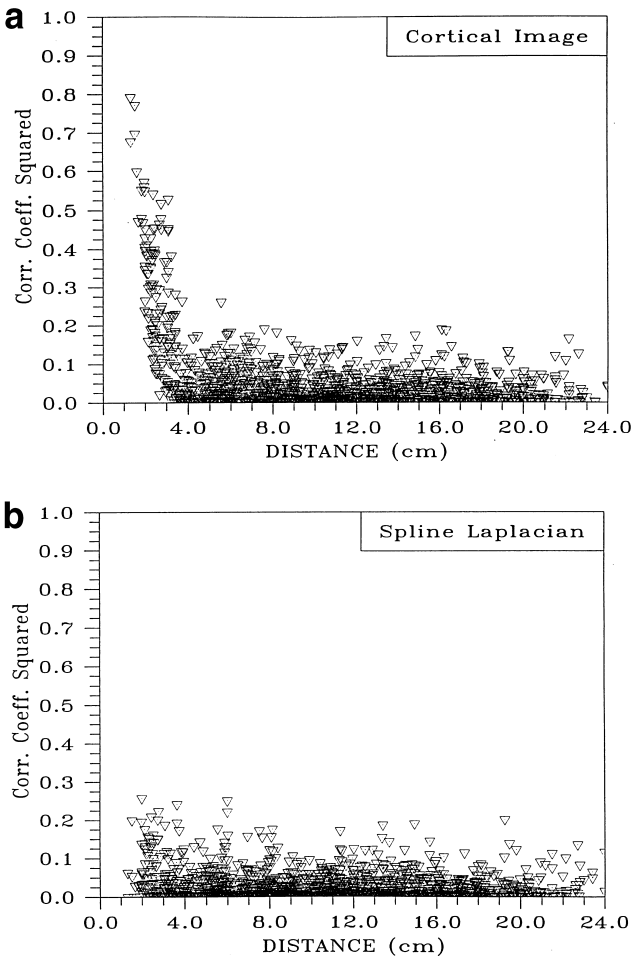

Fig. 5. (a) Simulated, squared correlation coefficients are plotted versus surface distance as in Figs. 3 and 4, except here surface potentials are first passed through an algorithm which uses the three sphere head model to estimate dura potential (Melbourne 'cortical imaging'). Thus, estimates of coherencies that would be recorded by large electrodes on the dura surface when generated by uncorrelated, uniformly distributed cortical dipoles are obtained. Short-range correlations are due to effects of volume conduction and smoothing of the cortical image estimate (a smoothing parameter of 10^{-08} is used here). The squared correlations are relatively small at distances greater than about 4 cm. Non-zero correlations at larger distances are mainly due to statistical fluctuations (for 60 averages). When 500 averages are used, nearly all squared correlation coefficients are less than 0.1 at distances greater than 4 cm; i.e. volume conduction and reference electrode effects are predicted to be very small. (b) Similar to (a) except calculated surface potentials are first passed through the New Orleans spline-Laplacian which also estimates dura surface potential, but requires no head model (other than the assumed shape of the outer surface). The resulting correlations due to random sources are slightly smaller than those obtained with Melbourne cortical imaging (due mostly to less smoothing). When 500 rather than 60 averages are used in simulations, statistical fluctuation is reduced so that nearly all squared correlations due to random sources are less than 0.05 at distances greater than 3 cm (Nunez, 1995). Thus, erroneous correlation due to volume conduction is very small. Erroneous correlation due to the reference is, of course, identically zero for the Laplacian estimate.

(6) Subtract expected coherence of scalp potentials due only to uncorrelated neural sources ('random coherence') from non-cephalic reference coherence to form 'reduced coherence' (Nunez, 1995).

Reduced coherence =

$$\text{(Measured coherence)} - \text{(Random coherence)} \qquad (12)$$

Random coherence is defined here as the correlation coefficient (squared) between potentials at pairs of scalp locations due to distributed, uncorrelated brain sources at fixed depth; it is a function only of surface separation distance in spherically symmetric head models. Random coherence was estimated using simulations of 500 source distributions, each consisting of 4200 different uncorrelated, uniformly distributed sources in a 3 concentric spheres model of the head with different reference locations (Nunez, 1995). These results were later supported with an analytic solution based on a similar volume conductor model, but potentials were referenced to infinity (Srinivasan, 1995, 1997). The analytic 'random coherencies' for scalp potential and Laplacian measures for uncorrelated cortical sources were expressed in terms of infinite sums of spherical harmonics. These theoretical and simulated correlations are plotted versus electrode separation distance in Fig. 6. To combine the analytic and simulation methods and to avoid complicated mathematics, rough estimates of random coherence may be obtained from

$$\text{Random coherence} = \exp[(1-x)/a] \quad x > 1 \qquad (13)$$

The parameter a is roughly in the range of 3–5 cm. Larger values of a provide a better fit to the heavy line in Fig. 6, which includes some reference contribution and random scatter in the 64 spatial samples (Nunez, 1995). Smaller a values correspond more closely to the analytic estimate of random coherence, in which potentials are referenced to infinity and the effective number of source distributions is infinite (Srinivasan, 1995). Here x is distance measured along the scalp in centimeters, and eqn (13) may be applied to all electrode separations greater than 1 cm. By definition, reduced coherence is set to zero when eqn (12) yields negative values. This simply means that when center-to-center electrode separation is too small, we cannot easily distinguish volume conduction from genuine underlying source coherence. For example, in our experimental study the electrode separation between F3 and Fz is 6.7 cm. Fig. 6 yields a random coherence of about 0.2–0.3 for this separation; any measured coherence lower than this value could easily be due only to volume conduction. One measured alpha rhythm coherence value between this pair of locations was 0.9 so that reduced coherence was in the range 0.6–0.7, presumably due to some combination of underlying source coherency and (possible) neck reference effect. In another example, measured coherence between F3 and T4 was 0.8. These locations are separated by 20.6 cm, corresponding to small random coherency. Thus our

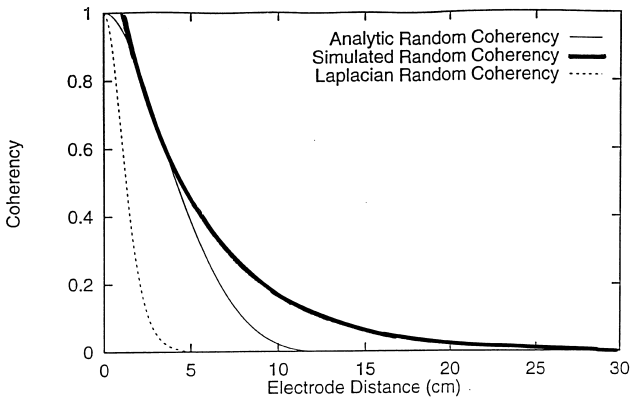

Fig. 6. Estimates of scalp coherency due to random cortical sources for the analytic scalp Laplacian (dashed line), analytic scalp potential (light solid line), and a rough fit to the simulated squared correlations in Fig. 3b (heavy solid line) are shown. The analytic solutions involve expansions of scalp potential and Laplacian in spherical harmonics plus stochastic field theory considerations (Srinivasan, 1995; Srinivasan et al., 1997). Analytic and simulated correlations do not agree exactly because analytic solutions assume the following: potentials are referenced to infinity (no reference effects), sampling is continuous over the surface (rather than 64 discrete points), and the effective number of source distributions used in averages is infinite (rather than 60 or 500). The analytic potential correlations show a small rise at large distances (not plotted) somewhat similar (but with smaller rise) to the average reference simulations of Fig. 4b.

measured coherence of 0.8 is close to reduced coherence for these distant electrodes.

Random coherence is based on the assumption of a large number of widely distributed, random cortical sources (radial dipoles) at a depth of 1.4 cm. It is insensitive to spherically symmetric head model changes, but could yield misleading results (e.g. erroneous high or low reduced coherence) in non-homogeneous or anisotropic heads, when reference effects are substantial, or if scalp potentials are dominated by a few isolated cortical source regions, tangential dipoles or by deep sources. Deeper sources will generally produce larger random coherence at large distances, i.e. larger values of the parameter *a*. For these reasons, eqn (13) should be used conservatively; i.e. random and reduced coherency should be viewed as idealized concepts that are appropriate for use in combination with other coherency measures. However, eqn (13) with the parameter *a* equal to 3 or 4 cm probably provides a reasonable estimate of the minimum random coherency that occurs for widely distributed, uncorrelated cortical sources. Furthermore, our studies of awake and sleep states show that, at frequencies of minimum coherence, coherence falls off with distance in a manner well approximated by eqn (13) with *a* in the range 3–5 cm.

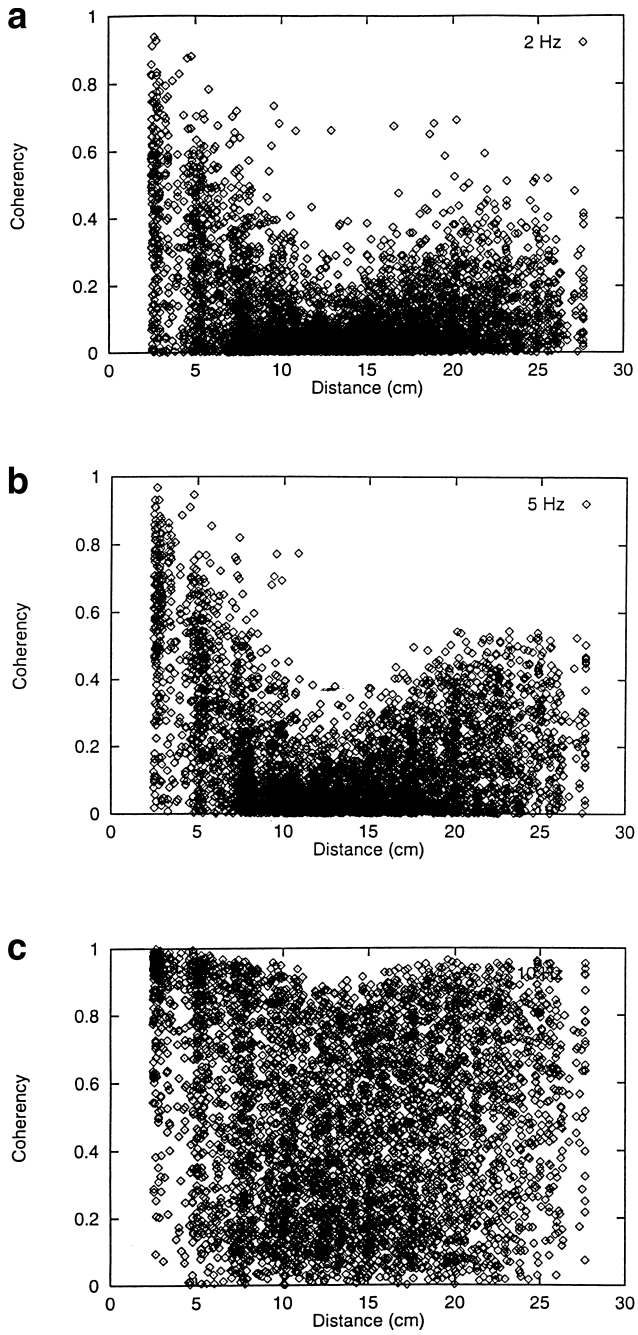

Fig. 7. Coherency versus distance plots calculated from 60 s of 128 channel, eyes-closed, resting EEG data recorded in Eugene from a 22 year old, normal male subject. The potentials are recorded with respect to a vertex reference and then average-referenced before calculating coherencies. Coherencies are calculated using 129 channels by setting the vertex channel (129) to zero in the original data and then including it in the average reference calculation. Thus, the vertex channel is the estimated reference signal obtained by averaging the other 128 channels (with a sign change). Coherencies between each electrode pair ($129 \times 128/2 = 8256$) are plotted versus electrode separation distance in a manner similar to the simulations of Figs. 3–5 (especially the average reference simulation, Fig. 4b). The main difference between EEG and simulated coherencies is that the latter are independent of frequency since all simulated sources are random and volume conduction is frequency-independent. By contrast, EEG sources have frequency-dependent correlations; 1 s epochs are Fourier-transformed so that 1 Hz frequency resolution is obtained. (a) 2 Hz coherency versus electrode separation distance. (b) 5 Hz coherency versus distance, obtained from the same 60 epochs. (c) 10 Hz coherency versus distance obtained from the same 60 epochs. The strong frequency dependence of these experimental coherencies is believed caused by large differences in moderate to long range neocortical source coherencies at different frequencies.

The connections between our simulations and experimental EEG data are illustrated in Part II (Nunez et al., 1997) and in Figs. 7 and 8. These 128 channel data were recorded in Eugene from a 22 year old, normal male subject, resting with eyes closed for 60 s. The potentials were recorded with respect to a vertex reference and then average-referenced before calculating coherency. Coherencies between each electrode pair ($129 \times 128/2 = 8256$) are plotted versus electrode separation distance in Figs. 7 and 8 in a manner similar to the simulations of Figs. 3–5. These EEG data show qualitative behavior observed in all normal subjects studied in Eugene and Melbourne. That is, high eyes-closed coherencies are obtained near the peak alpha frequency (Fig. 7c) and much lower eyes-closed coherencies occur in delta, theta, and beta bands. A partial exception occurs near 20 Hz (Fig. 8b), where relatively high coherencies may occur, possibly due to the presence of (phase locked) harmonics of the alpha rhythm (Nunez, 1981). Eyes-open coherencies in the alpha band (and perhaps to a lesser extent in other bands) are lower (not shown). The U-shaped behavior, roughly matching the average reference simulation of Fig. 4b, is clearly evident in all but the 10 Hz plot, for which the underlying source dynamics appears to be strongly correlated. Thus, we observe semi-quantitative agreement between the simulations and EEG data.

The use of reduced rather than measured coherency can have substantial impact on coherency confidence intervals when electrodes are closer than about 5 or 10 cm. For example, suppose reference coherence measured between electrodes separated by about 5 cm and based on 60 epoch averages is 0.8. The 95% coherence confidence interval is 0.74–0.87. However, the reduced coherence estimated from Fig. 6 is about ($0.8 - 0.4 = 0.4$), with a corresponding 95% confidence interval of 0.30–0.61. This latter estimate presents a quite different (and probably more accurate) picture of the uncertainty in underlying neocortical source coherency. Reduced coherence can also have a substantial impact on our physiological interpretation of brain state changes. Suppose, for example, that a brain state change corresponds to a reference coherence decrease from 0.8 to 0.7 between the same two electrodes (assuming very long averaging periods so that confidence intervals are narrow), i.e. a 12.5% decrease in reference coherence. The corresponding decrease in reduced coherence is from about 0.4 to 0.3, or 25%, suggesting a more robust reduction in underlying source coherency associated with the brain state change. These examples illustrate a mixture of good and bad news for quantifying brain state changes with coherence estimates.

5. Summary of reference contributions to EEG coherence

Even with a perfect head model, we cannot list general rules about reference contributions to coherence without knowing source locations and correlations in advance. However, our simulations of widely distributed, uncorrelated radial dipole sources, located in the upper half sphere of the 3 sphere model are in semi- quantitative agreement with EEG coherency fall-off with distance in the following

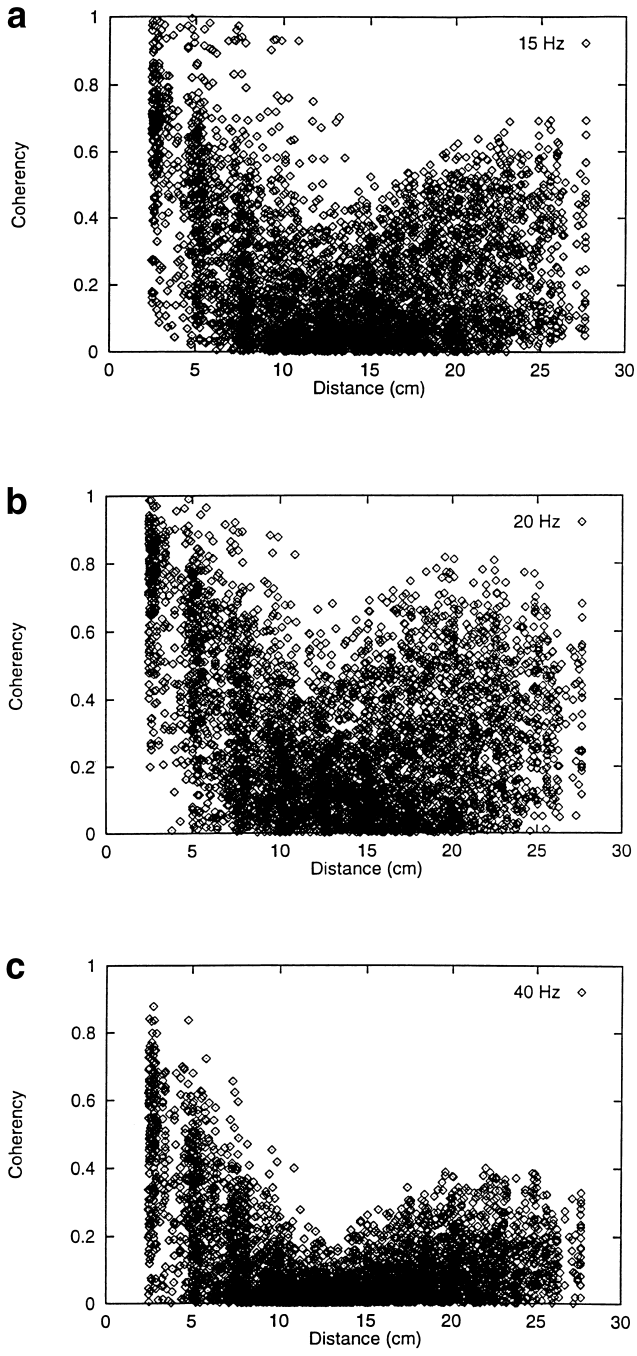

Fig. 8. Coherency versus distance plots calculated from the same 60 s of data used in Fig. 7. (a) 15 Hz coherency versus distance plot. (b) 20 Hz coherency versus distance plot; some contribution from the alpha rhythm harmonic is suggested. (c) 40 Hz coherency versus distance; this plot is fairly close to the average reference simulation using uncorrelated sources shown in b. Thus, intermediate and long range source coherencies are believed to be small at 40 Hz. Coherencies tend to fall off progressively at frequencies above 10 Hz, except for somewhat higher coherencies at alpha harmonics.

sense. In both awake and sleep data, there are certain brain states and frequencies for which coherency is minimal, suggesting uncorrelated or weakly correlated sources. These data are discussed in more detail in Part II (Nunez et al., 1997). For now, we list the following tentative 'rules of head', resulting from comparisons of EEG coherence estimates obtained with different references and from simulated data for which comparisons with reference-free (infinity reference) coherency were obtained.

(1) The averaged mastoids reference typically adds from 0.1 to 0.3 to coherence estimates at intermediate distances (roughly 5–15 cm). The largest changes occur for interhemispheric coherency, especially for electrode pairs close to reference locations. The effect on intrahemispheric coherency is much smaller, typically less than 0.1. One set of our simulations was based the 128 sample locations of the geodesic sensor net, which has 50 electrode positions near or below the plane of mesial cortex. Comparison of simulated average mastoid coherency with infinity-reference coherency showed that 37% changed by more than 0.1; however, only 18% of intrahemispheric coherencies changed by more than 0.1. These figures may present an overly pessimistic view of linked mastoids recordings since infinity-referenced coherency is not the 'gold standard'. Rather, it is strongly inflated by volume conduction. In this context, we note that, by contrast to average reference or infinity-referenced coherency, mastoid-linked coherency is typically less than 0.1 at distances greater than 15 cm, suggesting that the linked mastoid reference serves to cancel some of the volume conduction effect at large distances.

(2) Simulations using the geodesic sensor net electrode locations (128) show that all differences between average reference and infinity-referenced coherencies were less than 0.1. When only the 78 electrode locations above the mesial plane were used, the corresponding value was 11%. Simulations using the 10–20 system also yielded an 11% difference. However, comparisons of simulated average reference versus mastoid-linked reference did not correspond closely to corresponding results obtained in awake EEG (for which the infinity-reference is not available). This suggests reference contributions from deeper sources (quite possibly mesial cortex), correlated sources, anisotropic/non-homogeneous volume conduction, or some combination thereof.

6. Cortical image and surface Laplacian estimates of cortical potential

We have demonstrated a close theoretical connection between surface Laplacian and dura potential. The surface Laplacian estimates local, normal skull current, thereby taking advantage of the fact that the skull, which smears potential, focuses intracranial current (Nunez, 1981; Katznelson, 1981). Cortical image algorithms use a volume conductor model of the head to estimate dura potential (Cadusch et al., 1992; reviewed in Nunez et al., 1994). Analytic Laplacian estimates underlying cortical potential with a bias that is much smaller than scalp potential bias (Srinivasan et al., 1996). The Melbourne cortical image algorithm provides a similar estimate. Analytic Laplacians can only be estimated from experimental data; such estimates depend critically on electrode density and spline algorithm (Srinivasan et al., 1996). Nearest-neighbor Laplacian estimates (e.g. Hjorth, 1975) are easy to implement and have several practical EEG uses, but provide only very crude estimates of cortical potential. For this reason, it is very misleading to apply the general labels 'Laplacian' or 'CSD' to both spline and nearest-neighbor Laplacian estimates.

By contrast to nearest-neighbor methods, global spline-Laplacian and cortical imaging algorithms require sophisticated mathematical and programming development (Perrin et al., 1987; Pascual-Marqui et al., 1988; Nunez, 1988, 1989, 1990; Nunez et al., 1991; Babiloni et al., 1995). When applied with dense electrode arrays (typically 48–128 electrodes), they provide excellent estimates of inner surface potentials in spherical (Perrin et al., 1989; Nunez, 1991), general ellipsoidal (Law et al., 1993), or MRI-generated head models (Le et al., 1994; Babiloni et al., 1996). Since at least some of these methods appear to be robust with respect to head model errors, and theoretical accuracy is so much better than that obtained with raw scalp potential, a reasonable conjecture is that spline-Laplacian and cortical image estimates actually do provide substantially improved accuracy in most EEG experiments. However, both methods act as bandpass spatial filters which may remove genuine source activity associated with very low spatial frequencies, which the algorithms cannot distinguish from volume conduction. Thus, Laplacian and cortical image estimates should supplement, but generally not replace, raw potential measurements. Spline-Laplacians appear to be more robust to head model errors, but cortical image has more potential to take advantage of further improvements in head model accuracy (Le and Gevins, 1993; Gevins and Cutillo, 1995). We focus here mostly on cortical image coherency estimates which can be computed faster; however, the associated spline-Laplacian coherency issues are very similar.

7. Cortical image and Laplacian coherency estimates

Since global spline-Laplacian or cortical imaging algorithms appear to provide much more accurate estimates of dura potential than can be obtained with only raw scalp potential measurements, such methods might seem to finally solve the problem of erroneous high coherency due to volume conduction. However, the situation is not so simple and requires further discussion of spatial filtering effects.

It is often convenient to view spatial-temporal EEG patterns in terms of 2D or 3D Fourier transforms. Such patterns are expressed in terms of temporal (w) and spatial (k) frequencies, corresponding to one or two spatial coordinates on the dura surface. The squared Fourier transform (in time and

space) of dura surface potentials is called the spectral density function of dura dynamics, or $G_d(w,k)$. Such transformations are useful partly because the head volume conductor selectively filters parts of the spatial spectrum, depending on type of recording (Nunez, 1981, 1988, 1995). By contrast, the volume conductor does not directly filter temporal frequencies, as demonstrated with implanted dipole generators of variable frequency (Cooper et al., 1965). Rather, differences of waveforms (and temporal frequency spectra) between scalp and underlying cortex (Pfurtscheller and Cooper, 1975; Nunez, 1981) are believed to result indirectly from typical neocortical dynamic behavior; that is, high temporal frequencies on cortex tend to occur with high spatial frequencies, as suggested by several linear approximations to essentially non-linear theoretical models of neocortical dynamics (van Rotterdam et al., 1982; Ingber, 1995; Nunez, 1981, 1989, 1995). Direct experimental evidence for this effect for eyes open and eyes closed spontaneous EEG has been obtained (Nunez, 1974, 1995; Shaw, 1991). In fact, nearly any neocortical dynamic theory (linear or nonlinear) can be expected to predict certain preferred ranges for $G_d(w,k)$ on the dura surface, corresponding to 'mountain ranges' in 3D plots of $G_d(w,k)$. In the special case of linear waves, the equations for ridges across a mountain range, $w = w(k)$, are called 'dispersion relations'. The alternative to mountains is spatial-temporal white noise, corresponding to relatively flat $G_d(w,k)$ functions. Whatever the nature of the function $G_s(w,k)$, the high spatial frequency (k) portion must be filtered out between dura and scalp. Our EEG experiments allow crude estimates of the corresponding scalp spectral density function $G_s(w,k)$, which confirms that very little power occurs at high spatial frequencies (Nunez, 1974, 1981, 1995; Shaw, 1991).

Standard reference, average reference, bipolar, and a variety of Laplacian and cortical imaging methods each provide distinct spatial filtering of cortical potentials (Nunez, 1981, 1988, 1995, Srinivasan, 1995, 1996). The usual reference recordings yield extreme, spatially low pass versions of dura potential. Average reference and bipolar (perhaps 2–3 cm electrode spacing) methods extend the range to higher spatial frequencies, while partly removing signals with near zero spatial frequency. Spline-Laplacian and cortical imaging algorithms provide bandpass spatial filtering of $G_s(w,k)$ designed to match expected volume conductor properties. For example, very high spatial frequencies are removed by our algorithms based on spatial sampling limitations and the belief that very high intracranial spatial frequencies (k) must be filtered out by the head volume conductor. Thus, any such signals measured on the scalp are believed to be mostly artifact. Interpretation of very low spatial frequencies is more difficult. Such low spatial frequency signals must be partly removed to effectively cancel volume conduction; however, such action necessarily filters low spatial frequency signals from neural sources. We are not able to fully distinguish these potential contributions to low spatial frequencies without a perfect head model. This dilemma is analogous to that raised by temporal filtering with analog filters in EEG recording devices. That is, we typically remove EEG frequencies below about 0.5 Hz from $G_s(w,k)$ because of large artifact contribution at low temporal frequencies, even though such action may also remove important brain signals.

Laplacian and cortical image algorithms may filter out brain signals $G_d(w,k)$ at low spatial frequencies that have high coherence, thereby yielding 'erroneous' low coherence estimates (Nunez, 1995). We use quotes because such estimates are not wrong, rather they are limited to signals with power at intermediate spatial frequencies. In other words, raw scalp potential coherency involves cross spectral comparisons between large cortical regions. Such regions can easily involve 100 cm^2 or more of cortical gyri in the neighborhood of each electrode, even if reference electrode effects are negligible (Nunez, 1988). By contrast, spline-Laplacian coherency scales for the same pairs of electrodes are smaller and more dependent on electrode density. A reasonable estimate is that perhaps to 10–30 cm^2 of gyri surface (plus local sulci contributions) near each electrode contribute most of the recorded signal in the case of 2–3 cm electrode spacing (Nunez et al., 1994, 1995).

Very simplistic views of neocortical sources, for example models consisting of a few isolated 'generators' near each 'recording' electrode, imply that raw potential and Laplacian/cortical image coherency should be similar. However, complex dynamic views of neocortex, with distributed sources undergoing non-linear interactions at multiple scales, suggests that coherencies measured at different scales could behave quite differently. These arguments suggest that coherencies obtained with reference, average reference, bipolar, and various Laplacian or cortical imaging algorithms are partly independent measures which apply to different, but overlapping, parts of the spatial spectrum of cortical source activity or $G_d(w,k)$. A critical question in many EEG studies is, 'which coherency measures provide the most robust indicators of clinical or cognitive state?' This question must evidently be answered experimentally for each study. Thus, ideally, multiple coherency measures should be obtained in clinical or cognitive studies. Since most methods involve computer transformations of existing data, all but the Laplacian or cortical imaging approaches, which require more sophisticated algorithms and perhaps 48–128 electrodes, are easy to implement.

8. Erroneous high coherency produced by global spline algorithms?

Substantial erroneous high coherency estimates were attributed to a global, spherical spline-Laplacian algorithm, based on simulation studies and comparisons with Hjorth-Laplacian estimates of EEG data (Biggins et al., 1991). Since spline-Laplacian estimates (in contrast to Hjorth-

Laplacians) at each electrode site depend on potentials recorded at every electrode, such algorithmic effects are theoretically possible. However, we were initially puzzled by the apparent large magnitude of these effects since our global spline algorithm (which is based on interpolation in 3D space rather than on spherical surfaces) is apparently very effective at resolving local cortical source distributions at the 2–3 cm scale (Nunez et al., 1994). In particular, our simulation studies using a layered spherical model of the head show that the calculated scalp spline-Laplacian correlation coefficients (squared) due to uncorrelated cortical sources fall to values less than about 0.05–0.1 at electrode separation distances greater than 3 cm (Nunez, 1995). Furthermore, our nearest-neighbor (Hjorth generalization for unequal electrode spacing) and global spline-Laplacian estimates of 10 Hz alpha coherency yield similar magnitudes with no evidence of large algorithmic contamination of 3D global splines.

In simulation studies, the accuracy of spline-Laplacian estimates must be independent of temporal frequency unless non-random relationships between spatial and temporal properties are artificially created in the simulated data. In fact, spline algorithms can be applied either to potential time slices or to the Fourier coefficients obtained from transformed potential waveforms. Any frequency dependence of spline algorithm accuracy applied to EEG data can only be an indirect result of differences in spatial properties over the temporal frequency band, i.e. 'mountain ranges' in 3D plots of $G_s(w,k)$. For example, the 10 Hz alpha spectral peak occurs with relatively low spatial frequencies (k). If higher temporal frequencies of intracranial source dynamics are associated with higher spatial frequencies, coherency estimates of higher temporal frequency scalp potentials may be less accurate. In order to study such effects on alpha rhythm, we formed 4 local (12 electrodes), independent splines at electrode positions P3, P4, F3, and F4. Laplacian coherence spectra between electrode pairs obtained with the local splines were compared with equivalent spectra obtained with our global spline in 64 channel, eyes-closed data recorded in Melbourne (Nunez, 1995; Srinivasan et al., 1996). Since these two methods provide somewhat different spatial filtering of intracranial source activity, we cannot expect exact agreement. However, the equivalent spectra (1–30 Hz) were similar; e.g. coherency discrepancies were nearly all less than 0.1. In the case of the largest discrepancy (F3:F4), global estimates were actually somewhat lower than local estimates (for which the putative algorithmic inflation of coherence estimates is not possible).

Perrin (1992) pointed out that the equation for the spherical spline-Laplacian used by the Biggins group was incorrect. They replied with a modified study showing somewhat reduced, but still large, erroneous coherency estimates from their Laplacian algorithm (Biggins et al., 1992). We consider some possible reasons for the discrepancy between these latter results and the data reported here. The main difference between the two simulation studies is that we calculated estimated scalp potentials due to 4200 uncorrelated, cortical dipoles using a 3 sphere model of the head. As a result of volume conduction, the resulting scalp potentials are smooth and correlated (moderate to high correlations at distances up to roughly 8–10 cm). Application of the spline-Laplacian then removes most of the scalp correlation at distances larger than about 3 cm. By contrast, the Biggins group simulation did not use a volume conductor model; they simply used spatial white noise (random numbers generated for each electrode site). Thus, their signals necessarily contained substantial power at very high spatial frequencies. Much of this power evidently occurs at scalp spatial frequencies that are too high to be caused by intracranial sources, i.e. an unrealistic $G_s(w,k)$. Some of this power is essentially spatially aliased in simulations. We do not believe this is an appropriate test for spline-Laplacians, which attempt to estimate second spatial derivatives of relatively smooth functions. Another difference is that of the spline algorithms; the Biggins and Perrin groups use interpolation on a spherical surface. We interpolate in 3D space (Law et al., 1993), although it is unlikely that this accounts for major differences between the two simulation studies (Pascual-Marqui, 1993).

Differences between our spline-Laplacian simulations and those of the Biggins group are shown in Figs. 9 and 10. Fig. 9a shows the squared correlation coefficient of simulated scalp potential as a function of distance; Fig. 9b is the equivalent scalp spline-Laplacian plot. These are identical to the simulations depicted in Figs. 3b and Fig. 5b, respectively, except that 200 rather than 60 source distributions were used to estimate correlations. Fig. 10a shows an equivalent simulation with random numbers (no head model used to calculate scalp potentials, equivalent to correlations of actual sources). Fig. 10b shows the squared correlation coefficient obtained by passing random numbers through our spline-Laplacian, as apparently done by the Biggins group. The simulation of Fig. 9a shows that volume conduction causes random sources to produce moderate to strong scalp potential correlations at distances less than about 8–12 cm. Fig. 9b shows that the equivalent spline-Laplacian correlations (calculated from the simulated scalp potentials at 64 locations) are relatively small (all but one less than 0.2). By contrast, Fig. 10b shows that random number input to the spline-Laplacian algorithm produces many squared correlation coefficients larger than 0.2 (unsquared correlation coefficient 0.45) due to the presence of high spatial frequencies in the random input. These arguments suggest that algorithmic inflation of correlations by spline-Laplacians is actually quite minimal when applied to realistic scalp potentials.

9. Partial coherence functions

Other useful measures are multiple and partial coherence functions (Bendat and Piersol, 1986). Partial coherence is

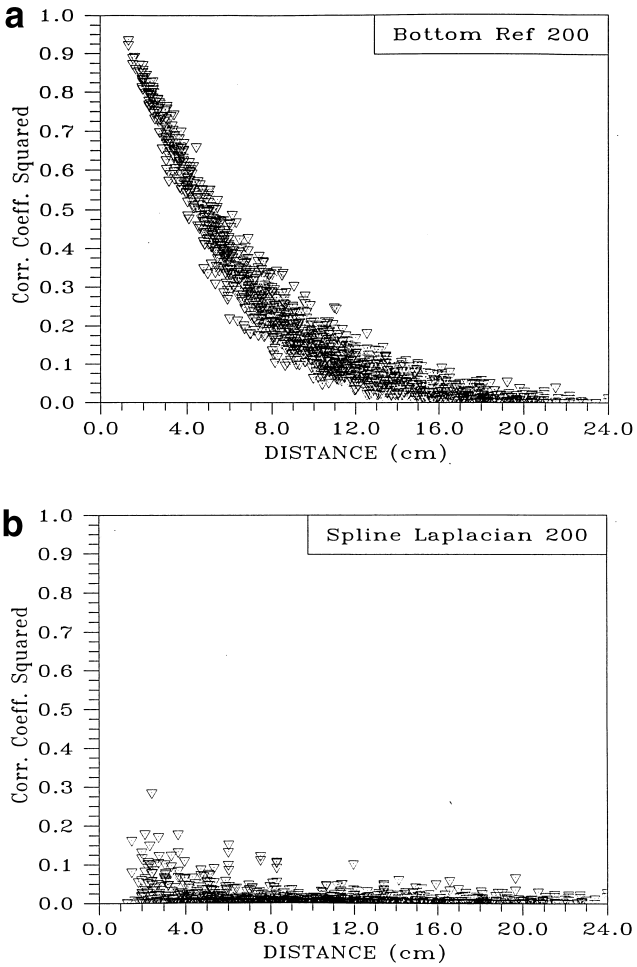

Fig. 9. (a) Simulated, squared correlation coefficients of outer surface potentials are plotted versus surface distance for the case of a reference at the bottom of the 3 sphere head model (crudely representing a neck of reference). Sources are assumed to be 4200 radial dipoles uniformly distributed over the upper surface of the inner sphere as in Fig. 3b, except 200 random source distributions are used here rather than 60. (b) The equivalent correlations of outer surface spline-Laplacians due to random cortical sources. Similar to Fig. 5b, but estimated with 200 source distributions.

discussed here briefly. Suppose the measured ordinary coherence between cortical regions (say D and E) is high. One might postulate that this high coherence occurs as a result of influence from a third region (F) on both D and E, rather than direct influence between D and E. One type of partial coherence function estimates the coherence between D and E after the influence of F on both D and E have been removed. Other partial coherence functions remove the influences of multiple regions (G, H, I,...) on D and E. For example, partial coherence was used to study the relative influences of corticocortical and thalamocortical influences on canine alpha rhythm (Lopes da Silva et al., 1980) and to distinguish between alpha and mu synchronization effects near sensorimotor cortex (Andrew and Pfurtscheller, 1996b; Florian and Pfurtscheller, 1996). Several issues must be addressed when using partial coherence in EEG. First, when scalp electrodes (say D and F or E and F) are close together, partial coherence estimates based on potentials (rather than Laplacian or cortical image estimates) mix dynamic influences and volume conduction effects, thereby making physiological interpretation very difficult. Second, one must decide on physiologic grounds which influences (G, H, I,…) on D and E to remove. For example, in one 21 channel study of waking and sleep data, the influences of all 17 other electrode sites on each pair of scalp locations were removed (Kaminski et al., 1995; Blinowska et al., 1996). Not surprisingly, the resulting partial coherencies were very small. This result is expected since the percentage of corticocortical and thalamocortical fibers entering any small or moderate sized cortical region D that also originate in a second region E is likely to be very small given the high interconnectivity of human neocortex. Thus, if we are able

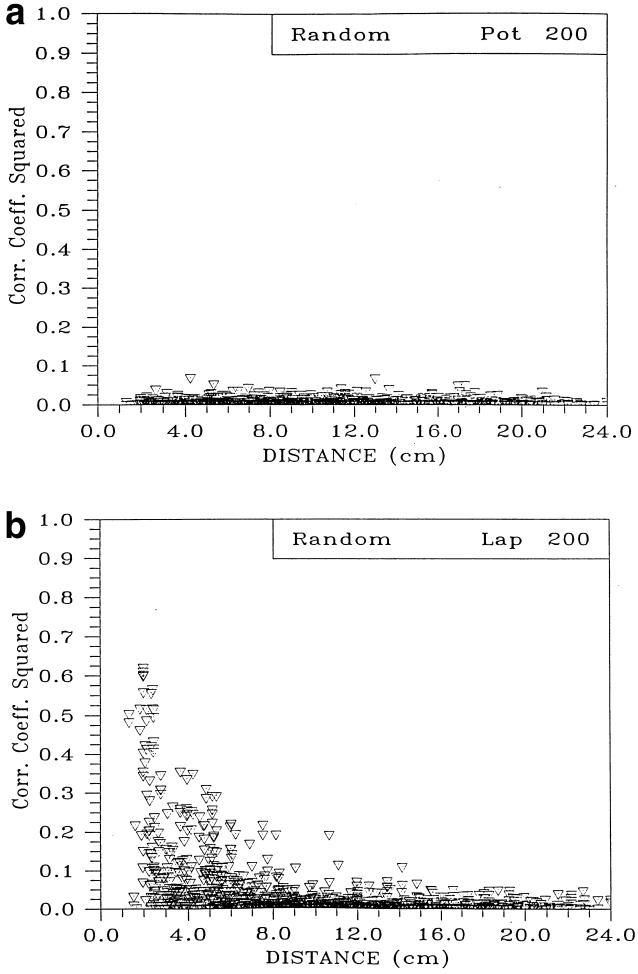

Fig. 10. (a) Simulation similar to Fig. 9a, except 200 sets of 4200 random numbers are used to estimate coherency. That is, no head model is used to calculate scalp potentials so the plot is equivalent to correlations of actual sources, which are zero at all distances. (b) Simulation similar to (a) except the same random numbers are submitted to our spline-Laplacian, a method similar to that used by the Biggins group. The simulation shows that random number input to the spline-Laplacian algorithm produces many squared correlation coefficients larger than 0.2 (unsquared correlation coefficient 0.45) due to the presence of high spatial frequencies in the random input (by contrast to the simulation of Fig. 9b which uses simulated scalp potentials as input to the spline-Laplacian).

to remove all indirect influences between D and E, we expect very small partial coherence between D and E. However, one main motivation for EEG coherence studies is to estimate changes in the amount and locations of dynamic coupling between regions with brain state changes, independent of the issue of actual coupling mechanisms.

Such dynamic couplings are of interest in medical and cognitive science because they often exhibit substantial, reproducible changes with brain state, as illustrated in Part II (Nunez et al., 1997). In this context, the underlying physiological mechanisms (which may be very difficult to determine) are of secondary importance to many EEG studies. To use an analogy to the dynamic global weather system, we may make use of robust correlation function coefficients between weather patterns in the western and eastern regions of the USA (time-delayed by several days). Ordinary correlation functions are very valuable, but if we were to use partial correlation functions to remove all but the direct influences (say between two cities D and E), we would expect to find no remaining correlations. We would then conclude that no pipelines through the earth directly connect D and E, hardly a surprising outcome. In summary, partial coherency is most useful when applied selectively to test specific neurophysiological hypotheses.

10. Concluding remarks

We consider reference, bipolar, average reference, cortical image, and Laplacian coherency measures as overlapping, but partly independent measures of neocortical source coherency. In a following paper (Nunez et al., 1997), we show that coherency measures at large spatial scales (the usual reference coherency) are more likely to exhibit consistency across different measures. Coherency measures at smaller scales (cortical image and spline-Laplacian) may show robust changes between states at fewer electrode pairs, but often with larger percentage changes between brain states at these more selective locations. That is, the average reference, cortical image, and reduced coherency usually behave in ways that are qualitatively similar to reference coherence when general comparisons between very large regions (lobal scales) are obtained; however, substantial differences between coherence measures occur for specific electrode pairs. This is particularly true for cortical image or spline-Laplacian coherency, measures expected to compare smaller cortical regions than reference potential coherency.

References

Andrew, C. and Pfurtscheller, G. Event-related coherence as a tool for studying dynamic interaction of brain regions. Electroenceph. clin. Neurophysiol., 1995, 98: 144–148.

Andrew, C. and Pfurtscheller, G. Dependence of coherence measurements on EEG derivation type. Med. Biol. Eng. Comput., 1996a, 34: 232–238.

Andrew, C. and Pfurtscheller, G. Coherence analysis of movement-related EEG. Proceedings of the Third International Hans Berger Congress, Jena, Germany, 3–6 October, 1996b.

Babiloni, F., Babiloni, C., Fattorini, L., Carducci, F., Onorati, P. and Urbano, A. Performances of surface Laplacian estimators: a study of simulated and real scalp potential distributions. Brain Topogr., 1995, 8: 35–45.

Babiloni, F., Babiloni, C., Carducci, F., Fattorini, L., Onorati, P. and Urbano, A. Spline Laplacian estimate of EEG potentials over a realistic magnetic resonance-constructed scalp surface model. Electroenceph. clin. Neurophysiol., 1996, 98: 363–373.

Bendat, J.S. and Piersol, A.G. Random Data. Analysis and Measurement Procedures, 2nd edn. Wiley, New York, 1986.

Biggins, C.A., Fein, G., Ratz, J. and Amir, A. Artifactually high coherence results from using spherical spline computation of scalp current density. Electroenceph. clin. Neurophysiol., 1991, 79: 413–419.

Biggins, C.A., Ezekiel, F. and Fein, G. Spline computation of scalp current density and coherence: a reply to Perrin. Electroenceph. clin. Neurophysiol., 1992, 83: 172–174.

Blinowska, K.J., Kaminski, M. and Szelenberger, W. Coherence and EEG activity propagation during sleep and wakefulness. Proceedings of the Third International Hans Berger Congress, Jena, Germany, 3–6 October, 1996.

Bullock, T.H., McClune, M.C., Achimowicz, J.Z., Iragui-Madoz, V.J., Duckrow, R.B. and Spencer, S.S. EEG coherence has structure in the millimeter domain: subdural and hippocampal recordings from epileptic patients. Electroenceph. clin. Neurophysiol., 1995a, 95: 161–177.

Bullock, T.H., McClune, M.C., Achimowicz, J.Z., Iragui-Madoz, V.J., Duckrow, R.B. and Spencer, S.S. Temporal fluctuations in coherence of brain waves. Proc. Natl. Acad. Sci. USA, 1995b, 92: 11568–11572.

Cooper, R., Winter, A.L., Crow, H.J. and Walter, W.G. Comparison of subcortical, cortical and scalp activity using chronically indwelling electrodes in man. Electroenceph. clin. Neurophysiol., 1965, 18: 217–228.

Cadusch, P.J., Breckon, W. and Silberstein, R.B. Spherical splines and the interpolation, deblurring and transformation of topographic EEG. Pan Pacific Workshop on Brain Electric and Magnetic Topography, Melbourne, 17–18 February, 1992.

de Munck, J.C., Vijn, P.C.M. and Lopes da Silva, F.H. A random dipole model for spontaneous activity. IEEE Trans. Biomed. Eng., 1992, 39: 791–804.

Essl, M. and Rappelsberger, P. Dependence of coherence using different recording techniques. Proceedings of the Third International Hans Berger Congress, Jena, Germany, 3–6 October, 1996.

Fein, G., Raz, J., Brown, F.F. and Merrin, E.L. Common reference coherence data are confounded by power and phase effects. Electroenceph. clin. Neurophysiol., 1988, 69: 581–584.

Florian, G. and Pfurtscheller, G. Changes of coherence during finger movement. Proceedings of the Third International Hans Berger Congress, Jena, Germany, 3–6 October, 1996.

Gevins, A.S. and Cutillo, B.A. Signals of cognition. In: F.H. Lopes da Silva (Ed.), Handbook of Electroencephalography and Clinical Neurophysiology, Vol. 2. Elsevier, Amsterdam, 1986, pp. 335–381.

Gevins, A.S. and Cutillo, B.A. Neuroelectric measures of mind. In: P.L. Nunez, Neocortical Dynamics and Human EEG Rhythms. Oxford University Press, New York, 1995, pp. 304–338.

Gevins, A., Brickett, P., Reutter, B. and Desmond, J. Seeing through the skull: advanced EEGs use MRIs to accurately measure cortical activity from the scalp. Brain Topogr., 1991, 4: 125–131.

Gotman, J. Interhemispheric interactions in seizures of focal onset: data from human intracranial recordings. Electroenceph. clin. Neurophysiol., 1987, 67: 120–133.

Hjorth, B. An on line transformation of EEG scalp potentials into orthogonal source derivations. Electroenceph. clin. Neurophysiol., 1975, 39: 526–530.

Ingber, L. Statistical mechanics of multiple scales of neocortical interactions In: P.L. Nunez, Neocortical Dynamics and Human EEG Rhythms. Oxford University Press, New York, 1995, pp. 628–681.

Kaminski, M., Blinowska, K. and Szelenberger, W. Investigation of coherence structure and EEG activity propagation during sleep. Acta Neurobiol. Exp., 1995, 55: 213–219.

Katznelson, R.D. EEG recording, electrode placement and aspects of generator localization. In: P.L. Nunez, Electric Fields of the Brain: The Neurophysics of EEG. Oxford University Press, New York, 1981, pp. 176–213.

Katznelson, R.D. Deterministic and stochastic field theoretic models in the neurophysics of EEG. Ph.D. Dissertation, University of California at San Diego, 1982.

Koeda, T., Knyazeva, M., Njiokiktjien, C., Jonkman, E.J., De Sonneville, L. and Vildavsky, V. The EEG in acallosal children. Coherence values in the resting state: left hemisphere compensatory mechanism? Electroenceph. clin. Neurophysiol., 1995, 95: 397–407.

Law, S.K., Nunez, P.L. and Wijesinghe, R.S. High resolution EEG using spline generated surface Laplacians on spherical and ellipsoidal surfaces. IEEE Trans. Biomed. Eng., 1993, 40: 145–153.

Le, J. and Gevins, A.S. Method to reduce blur distortion from EEGs using a realistic head model. IEEE Trans. Biomed. Eng., 1993, 40: 517–528.

Le, J., Vinod, M. and Gevins, A. Local estimate of surface Laplacian derivation on a realistically shaped scalp surface and its performance on noisy data. Electroenceph. clin. Neurophysiol., 1994, 92: 433–441.

Lieb, J.P., Hoque, K., Skomer, C.E. and Song, X.W. Inter-hemispheric propagation of human mesial temporal lobe seizures: a coherence/phase analysis. Electroenceph. clin. Neurophysiol., 1987, 67: 101–119.

Lopes da Silva, F.H., Vos, J.E., Mooibroek, J. and van Rotterdam, A. Partial coherence analysis of thalamic and cortical organization of rhythmic activity. In: G. Pfurtscheller, P. Busar, F.H. Lopes da Silva and H. Petsche (Eds.), Rhythmic EEG Activities and Cortical Functioning. Elsevier, Amsterdam, 1980, pp. 33–59.

Marosi, E., Harmony, T., S :ánchez, L., Becker, J., Bernal, J. and Reyes, A. Maturation of the coherence of EEG activity in normal and learning-disabled children. Electroenceph. clin. Neurophysiol., 1992, 83: 350–357.

Miller, G.A., Lutzenberger, W. and Elbert, T. The linked-reference issue in EEG and ERP recording. J. Psychophysiol., 1991, 5: 276–279.

Nielsen, T., Montplaisir, J. and Lassonde, M. Decreased interhemispheric EEG coherence during sleep in agenesis of the corpus callosum. Eur. Neurol., 1993, 33: 173–176.

Nunez, P.L. Wave-like properties of the alpha rhythm. IEEE Trans. Biomed. Eng., 1974, 21: 473–482.

Nunez, P.L. Electric Fields of the Brain: The Neurophysics of EEG. Oxford University Press, New York, 1981.

Nunez, P.L. Locating sources of the brain's electric and magnetic fields: some effects of inhomogeneity and multiple sources, with implications for the future. Human Factors and Organizational Systems Laboratory Technical Note 71-86-12, US Navy, San Diego, 1986.

Nunez, P.L. Spatial filtering and experimental strategies in EEG. In: D. Samson-Dollfus (Ed.), Functional Brain Imaging. Elsevier, Paris, 1988, pp. 196–209.

Nunez, P.L. Generation of human EEG by a combination of long and short range neocortical interactions. Brain Topogr., 1989, 1: 199–215.

Nunez, P.L. Physical principals and neurophysiological mechanisms underlying event related potentials. In: J. Rohnbaugh, R. Johnson, and R. Parasuraman (Eds.), Event-related Potentials of the Brain. Oxford University Press, New York, 1990.

Nunez, P.L. Comments on the paper by Miller, Lutzenberger and Elbert. J. Psychophysiol., 1991, 5: 279–280.

Nunez, P.L. Neocortical Dynamics and Human EEG Rhythms. Oxford University Press, New York, 1995.

Nunez, P.L. and Pilgreen, K.L. The spline-Laplacian in clinical neurophysiology: a method to improve EEG spatial resolution. J. Clin. Neurophysiol., 1991, 8: 397–413.

Nunez, P.L., Pilgreen, K.L., Westdorp, A.F., Law, S.K. and Nelson, A.V. A visual study of surface potentials and Laplacians due to distributed neocortical sources: computer simulations and evoked potentials. Brain Topogr., 1991, 4: 151–168.

Nunez, P.L., Silberstein, R.B., Cadiush, P.J., Wijesinghe, R.S., Westdorp, A.F. and Srinivasan, R. A theoretical and experimental study of high resolution EEG based on surface Laplacians and cortical imaging. Electroenceph. clin. Neurophysiol., 1994, 90: 40–57.

Nunez, P.L., Silberstein, R.B., Carpentar, M.R., Srinivasan, R., Wijesinghe, R.S., Tucker, D.M., Cadusch, P.J. and Wu, X. EEG coherency. II: Comparisons of multiple measures of EEG coherency differences between resting and cognitive states, Electroenceph. clin. Neurophysiol., 1997, submitted for publication.

Pascual-Marqui, R.D. The spherical spline Laplacian does not produce artifactually high coherencies: comments on two articles by Biggins et al. Electroenceph. clin. Neurophysiol., 1993, 87: 62–64.

Pascual-Marqui, R.D., Gonzalez-Andino, S.L., Valdes-Sosa, P.A. and Biscay-Lirio, R. Current source density estimation and interpolation based on the spherical harmonic Fourier expansion. Int. J. Neurosci., 1988, 43: 237–249.

Perrin, F. Comments on article by Biggens et al. Electroenceph. clin. Neurophysiol., 1992, 83: 171–172.

Perrin, F., Bertrand, O. and Pernier, J. Scalp current density mapping: value and estimation from potential data. IEEE Trans. Biomed. Eng., 1987, 34: 283–287.

Perrin, F., Pernier, J., Bertrand, O. and Echallier, J.F. Spherical spline for potential and current density mapping. Electroenceph. clin. Neurophysiol., 1989, 72: 184–187.

Petsche, H., Richter, P., Stein, A.V., Ethlinger S.C. and Filz, O. EEG coherence and musical thinking. Music Percept., 1993, 11: 117–152.

Pfurtscheller, G. and Cooper, R. Frequency dependence of the transmission of the EEG from cortex to scalp. Electroenceph. clin. Neurophysiol. 1975, 38: 93–96.

Pfurtscheller, G. and Berghold, A. Pattern of cortical activation during planning of voluntary movement. Electroenceph. clin. Neurophysiol, 1989, 72: 250–258.

Pfurtscheller, G. and Neuper, C. Simultaneous EEG 10 Hz desynchronization and 40 Hz synchronization during finger movements. Neurol. Rep., 1992, 3: 1057–1060.

Pfurtscheller, G., Neuper, C. and Berger, J. Source localization using event-related desynchronization (ERD) within the alpha band. Brain Topogr., 1994, 6: 269–275.

Pilgreen, K.L. Physiologic, medical, and cognitive correlates of electroencephalography. In: P.L. Nunez, Neocortical Dynamics and Human EEG Rhythms. Oxford University Press, New York, 1995, pp. 195–248.

Rappelsberger, P. and Petsche, H. Probability mapping: power and coherence analyses of cognitive processes. Brain Topogr., 1988, 1: 46–54.

Rush, S. and Driscoll, D.A. EEG electrode sensitivity: an application of reciprocity. IEEE Trans. Biomed. Eng., 1969, 16: 15–22.

Schack, B. and Krause, W. Dynamic power and coherence analysis of ultra short-term cognitive processes—a methodical study. Brain Topogr., 1995, 8: 127–136.

Schack, B., Haueisen, J., Krause, W., Grieszbach, G., Nowak, H. and Witte, H. Simultaneous EEG and MEG analysis of short-term cognitive processes. Proceedings of the Third International Hans Berger Congress, Jena, Germany, 3–6 October, 1996.

Shaw, G.R. Spherical harmonic analysis of the electroencephalogram. Ph.D. Dissertation, The University of Alberta, 1991.

Sidman, R.D. A method for simulating intracerebral potential fields. The cortical imaging technique. J. Clin. Neurophysiol., 1991, 8: 432–441.

Srinivasan, R. A theoretical and experimental study of neocortical dynamics. Ph.D. Dissertation, Tulane University, 1995.

Srinivasan, R., Nunez, P.L., Tucker, D.M., Silberstein, R.B. and Cadusch, P.J. Spatial sampling and filtering of EEG with spline Laplacians to

estimate cortical potentials. Brain Topogr., 1996, 8: 1–12.
Srinivasan, R., Nunez, P.L. and Silberstein, R.B. Spatial filtering and neocortical dynamics: estimates of EEG coherence. IEEE Trans. Biomed. Eng., 1997, submitted for publication.
Thatcher, R.W. and Walker, R.A. EEG coherence and intelligence in children. Electroenceph. clin. Neurophysiol., 1985, 61: 481–508.
Thatcher, R.W., Krause, P.J. and Hrybyk, M. Cortico-cortical associations and EEG coherence: a two-compartmental model. Electroenceph. clin. Neurophysiol., 1986, 64: 123–143.
Tucker, D.M., Dawson, S.L., Roth, D.L. and Penland, J.G. Regional changes in EEG power and coherence during cognition: intensive study of two individuals. Behav. Neurosci., 1985, 99: 564–577.
van Rotterdam, A., Lopes da Silva, F.H., van den Ende, J., Viergever, M.A. and Hermans, A.J. Model of the spatial-temporal characteristics of the alpha rhythm. Bull. Math. Biol., 1982, 44: 283–305.